P7.1 REAL-TIME CLOUD, RADIATION, AND AIRCRAFT ICING PARAMETERS FROM GOES OVER THE USA

Patrick Minnis, Louis Nguyen, William Smith, Jr., David Young
Atmospheric Sciences, NASA Langley Research Center, Hampton, VA 23681

Mandana Khaiyer, Rabindra Palikonda, Douglas Spangenberg, Dave Doelling, Dung Phan, Greg Nowicki, Kirk Ayers
AS&M, Inc., Hampton, VA 23666

Patrick W. Heck
CIMSS, University of Wisconsin-Madison, Madison, WI, USA 53706

Cory Wolff
NCAR, Boulder, CO, USA 80301

1. INTRODUCTION

New sensors and retrieval algorithms have facilitated the development of more quantitative uses for geostationary (GEO) satellite data in weather and climate. For weather applications such as data assimilation or air safety, near real-time processing is needed to produce datasets in a timely fashion. It requires not only fast data throughput, readily available on many computer systems, but good calibration of the sensors to ensure accuracy of the products. Reliable calibration, formerly a chronic problem for some GEO imager channels, can be readily acquired using the more commonly operating, well-calibrated research satellites (Minnis et al., 2002). Satellite-derived cloud and radiation products such as cloud phase or albedo have been available for a number of years from satellites devoted to climate studies but have been generated only sporadically from operational weather satellites. With improving forecast models and the ever-present need for air safety information, such products will be useful for model validation and assimilation and for diagnosing air-traffic hazards.

Minnis et al. (2001) adapted a set of algorithms used on low-Earth orbit satellite data for Earth radiation budget and cloud process studies to provide a variety of pixel-level products for the Atmospheric Radiation Measurement (ARM) Program over the central United States of America (USA) in near real-time. Smith et al. (2002, 2003) demonstrated that several of the derived products could be useful for diagnosing aircraft icing potential. Because icing can occur anywhere over the USA, the products should not be limited the central USA but should be available over the entire country. With the aid of the NASA Advanced Satellite Aviation-weather Products (ASAP) program, the ARM domain has recently been expanded to include the entire continental USA requiring the combination of 4-km data form both the East and West Geostationary Operational Environmental Satellites (GOES). This paper summarizes the current state of those products and their applicability to aircraft icing potential.

*Corresponding author address: Patrick Minnis, NASA Langley Research Center, MS 420, Hampton, VA 23681-2199. email: p.minnis@larc.nasa.gov.

2. DATA & METHODOLOGY

The USA domain covers 25°N - 50°N and 65°W - 125°W. Datasets used here include half-hourly GOES-10, and 12 4-km spectral radiances. The GOES-10 at 135°W measures radiances at 0.65, 3.9, 10.8, and 12 μm while the 12-μm channel on GOES-12 at 75°W was replaced with a 13.3-μm channel. GOES-12 data are analyzed over an area between 65°W and 105°W, while the GOES-10 data cover 90°W to 125°W. The results are stitched together at 99°W. The Rapid Update Cycle (RUC) analyses (Benjamin et al., 2004) provide hourly profiles of temperature and humidity at spatial resolutions of 40 and 20 km before and after April 2002, respectively. The RUC data are used to convert the retrieved cloud temperature Tc to cloud height z_c and correct radiances for atmospheric attenuation. Surface-type, clear-sky albedo, and surface emissivity maps are used to estimate the cloud-free radiances for a given scene as described by Minnis et al. (2001, 2004).

The analysis procedure is outlined in Fig. 1, where the green boxes indicate relatively fixed input parameters and the light blue denotes the input varying at each time step. The data are processed as tiles (1° region). After estimating the clear-sky radiances for each tile (gray boxes in center), each pixel is classified as clear or cloudy (tan box) based on a set of decision trees using all four channels. If clear pixels are found in the tile, they replace the original clear radiance field for the tile and are used to derive the cloud properties for each cloudy pixel. For each clear pixel, the algorithm

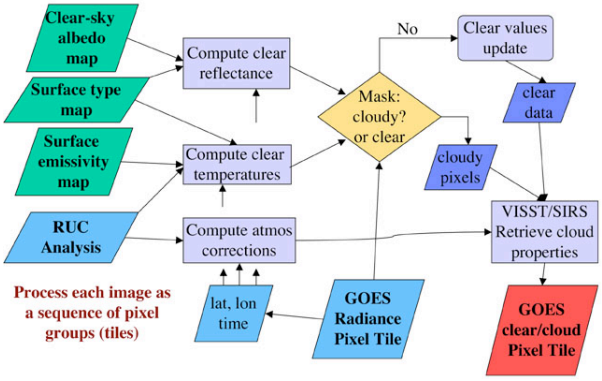

Fig. 1. Schematic real-time processing flow.

estimates surface skin temperature, the outgoing longwave radiation (OLR), and the clear-sky VIS and shortwave (ASW) albedos (not indicated in Fig. 1).

When the solar zenith angle *SZA* is less than 82° (daytime), cloudy pixels are analyzed with the visible infrared solar-infrared split-window technique (VISST; Minnis et al., 1995), which matches the observed values with theoretical models of cloud reflectance and emittance (Minnis et al. 1998). At night, the cloud properties are determined using the solar-infrared infrared split-window technique (SIST), an improved version of the 3-channel nighttime method of Minnis et al. (1995). It uses 3.9, 10.8, and 12.0-μm data for GOES-10 and only the first two channels for GOES-12. The methods estimate effective cloud temperature *Tc*, cloud height *z* and thickness *h*, phase, optical depth *OD*, effective droplet radius *re* or effective ice crystal diameter *De*, and LWP or ice water path *IWP*. Pixels with $Tc < 273$ K and identified as liquid water are designated as supercooled liquid (SLW) clouds. Other properties related to icing include *h*,*OD*, and *LWP*. Cloud thickness, used to find cloud base height, is estimated using the empirical parameterizations based on ARM cloud radar and satellite data (Chakrapani et al., 2001). The top-of-atmosphere VIS albedo, ASW, and OLR are also computed for each cloudy pixel. The results are output for each tile (red box in Fig. 1).

These results are then used to estimate the aircraft icing probability for each pixel in a tile. The potential for aircraft icing depends on many factors related to the particular aircraft and the weather conditions. Some aircraft will accumulate ice in certain conditions while other planes will remain ice-free in the same cloud. These aircraft-related factors are not considered here. A necessary condition for icing is the presence of supercooled liquid water, relatively large droplets, and/or large concentrations of droplets or high liquid water content (LWC). SLW can be discriminated from warm clouds using *Tc* while the concentration of large droplets should be related to *re*. LWC can be estimated as the ratio of LWP/*h*. However, since both LWP and *h* depend on *OD*, only LWP is used here as a proxy for LWC. Smith et al. (2002, 2003) found some weak positive dependencies of icing intensity on LWP and *re*, and a weak negative dependency on *Tc* using matched VISST and in situ aircraft data.

Minnis et al. (2004b) developed a probability based method to classify the icing potential for each pixel based on pilot reports (PIREPS). No pixels classified as cloudy with $Tc > 273$ K or $LWP < 40$ gm^{-2}, as clear, or as an ice cloud with $OD < 5$ are considered as icing potential candidates. Ice clouds with $OD > 5$ are considered as indeterminate pixels because the nature of any clouds below the ice cloud cannot be discerned. The approach estimates the icing probability for the remaining pixels is estimated as

$$IP = 0.147 \ln(LWP) - 0.084, \quad (1)$$

for $re = 5$ μm, and

$$IP = 0.138 \ln(LWP) - 0.024, \quad (2)$$

for $re = 16$ μm. Linear interpolation between the results of (1) and (2) are used for pixels with *re* between 5 and 16 μm. Pixels with larger or smaller values of *re* are assigned the appropriate extreme value. The intensity of icing is classified as light or moderate-severe if *LWP* is less or greater than 440 gm^{-2}, respectively. This approach to estimating the probability for icing is considered as a preliminary technique because it is based on only 11 days of PIREPS and GOES-12 data taken during February 2004. It will be evaluated using an additional 18 and 11 days of GOES-12 and 10 data, respectively.

3. RESULTS

Figure 2 shows an example of the USA results for GOES-10/12 imagery taken at 1845 UTC, 15 March 2004. The pseudocolor RGB image (Fig. 2a) reveals the various cloud types in a single image. In this type of image, red is assigned to the visible reflectance, the temperature difference between the 3.9 and 11-μm channels determines the green intensity, and the 11-μm temperature *T* provides the blue intensity on an inverse scale. Snow-free clear areas like much of the western USA and northern Mexico are green, blue, or tan while clear snow-covered areas such as Colorado, Wyoming, the Sierra Nevada Mountains, western Iowa, northern Minnesota, and Quebec are typically bright or dark pink. High clouds are generally white (e.g, Montana), grey (e.g., Sea of Cortez), or some shade of magenta (e.g., North Carolina to Michigan), while low or midlevel clouds are often white (e.g., Oregon) or a shade of peach or orange (e.g., Texas and Arkansas). The retrieved cloud phase image (Fig. 2b) shows clear areas in green, warm liquid water clouds in dark blue, SLW clouds in light blue, and ice clouds in red. Some of the scattered clouds over the western US are actually misclassified clear areas because the clear-sky albedo map has not yet been optimized for the GOES VIS spectral band or they occur near the edge of snow fields. SLW clouds cover nearly all of the northeastern USA. The derived values of *re* (Fig. 2c) are typically between 7 and 11 μm but greater values occur off the Washington coast and over southeastern Texas. In some overlapped conditions along the edges of ice clouds (e.g., Pennsylvania, Wisconsin) or for relatively thin clouds over snow (northern Nevada), the VISST often retrieves a large value of *re* because the 3.9-μm radiance is diminished due to absorption by ice in the form of large cirrus crystals or snow grains. The cloud *LWP* (Fig. 2e) reaches extremely high values, exceeding 400 gm^{-2}, around Lake Michigan and the Pacific Northwest. More commonly, *LWP* is less than 200 gm^{-2}. The cloud top heights (Fig. 1d) range between 8 and 10 km over northern Florida and in the Northwest. Most of the cloud tops are below 3 km. The bases (Fig.

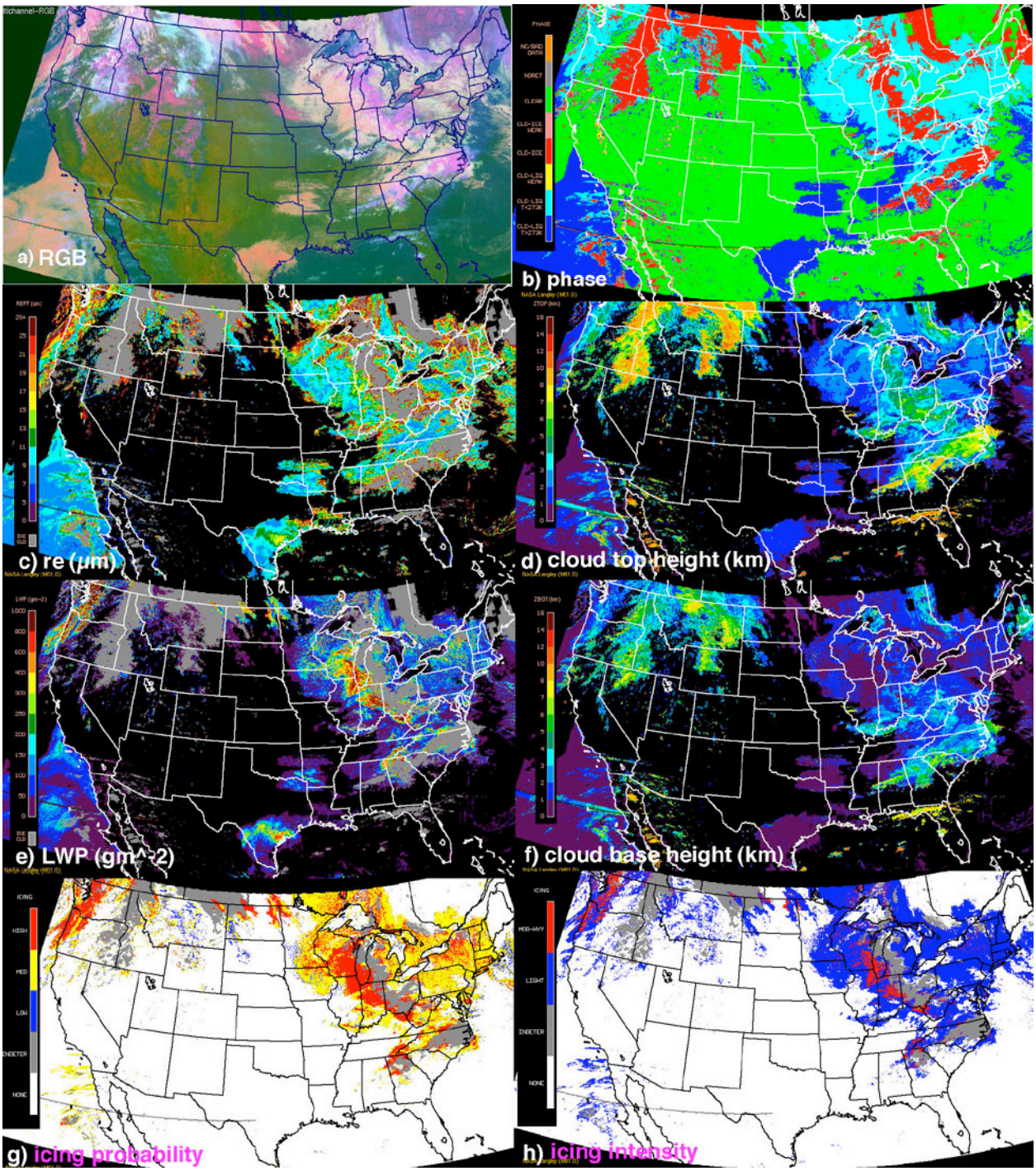

Fig. 2. Selected cloud and aircraft icing parameters from GOES10 and 12, 1845 UTC, 18 March 2004. Gray indicates ice clouds in (a) and (e) and indeterminate icing in (g) and (h). Color bar ranges: (b) dark blue, warm clouds; light blue, SLW; red or pink, ice clouds (c) 5 (blue) to 21 μm (red), > 21 μm, dark red; (d & f) 0 – 10 km (purple –red), 10 –16 km; (e) 0-300 gm^{-2}, purple to light green; 300 – 400 gm^{-2}, yellow; 400 – 1000 gm^{-2}, orange to dark red; (g) low – blue, medium – yellow, high – red; (h) low – blue, moderate/severe - red.

2f) for most of the low clouds are estimated at 1 km or less while the high cloud bases are between 3 and 7 km. Most of the SLW clouds have icing probabilities between low (0-33%) and medium (34-67%) with high (> 67%) probabilities around Lake Michigan. The medium-to-high values off the Baja coast are most likely an artifact of thin cirrus over warm low-level clouds (Fig. 2b) that are sometimes misinterpreted as SLW clouds. The potential icing intensity is generally light except in the Northwest and around Lake Michigan (Fig. 2h).

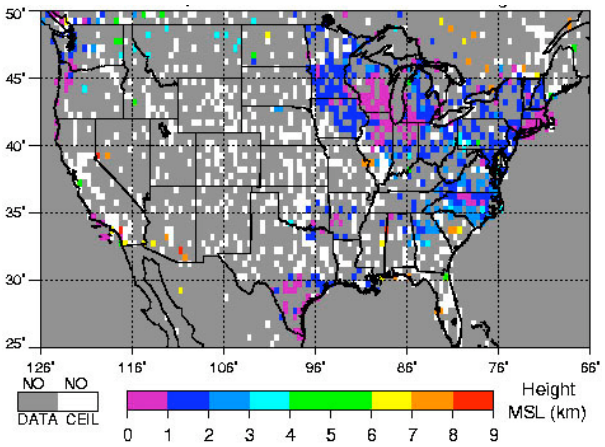

Fig. 3. Cloud base heights from ASOS ceilometers, 1900 UTC, 18 March 2004.

The cloud property and icing methodologies are currently being applied in near-real time to GOES-10 and 12 data every half hour during the daytime and hourly at night. The results from each satellite are available separately and stitched together at the URL, http://www-angler.larc.nasa.gov/satimage/products.html, in image or digital formats. The vertical extent of the potential icing clouds can be estimated from the cloud-top and base altitudes of the clouds.

4. DISCUSSION

The example results presented above serve as samples of the products currently being generated, but the algorithms used to derive each product are continually being updated as validation studies provide new information or advanced methods become available. Validation efforts have demonstrated that properties like cloud optical depth, particle size, and ice and liquid water path (e.g., Young et al., 1998; Dong et al., 2002; Min et al., 2004) are reasonably well correlated with and similar in magnitude to in situ and active remote sensing retrievals. The validations are continuing.

Figure 3 shows the cloud bases measured with the Automated Surface Observing Systems (ASOS) ceilometers at 1845 UTC, 18 March 2004. Many of the VISST cloud base heights in Fig. 2f are in relatively good agreement (± 0.5 km) with the ASOS data over many areas such as Texas, Wisconsin, New York, Washington, and Pennsylvania. In other areas where clouds are high or icing is indeterminate, the agreement is mixed. The bases are in good agreement over Florida, Idaho, and North Dakota, but not over Quebec, North Carolina, and Georgia. Over Quebec, the retrieved cloud tops are lower than the ASOS bases, indicating that the VISST is overestimating the cloud *OD* resulting in too little correction of *T* to determine *Tc*. This error is likely a result of the snow cover over Quebec, which causes a large uncertainty in the clear-sky albedo. On the other hand, the retrieved bases over the Southeast are a few kilometers higher than the ASOS values. These are the same areas classified as indeterminate by the icing algorithm because it is not possible to determine if a low cloud is below the high cloud observed form the satellite. The ASOS results indicate that a low cloud deck is present under the ice clouds and based on the properties of low clouds in the surrounding areas, significant icing potential is likely in those regions where the cloud base is too high relative to the ASOS. Thus, it appears that merging of the ceilometer data with the VISST results could be valuable for estimating the icing potential for indeterminate cases.

In situ data from a variety of field measurements as well as PIREPS have been used to validate the satellite icing measurements (Smith et al., 2002, 2003; Minnis et al., 2004b). For example, Smith et al. (2000) showed that when overlying cirrus clouds were absent, the VISST retrieved SLW in 98% of the PIREPS reports of positive icing indicating that the satellite can provide the first condition necessary to identify icing conditions. Determining the other conditions becomes more difficult. Thus, validation and improvement of the prototype algorithm has begun by comparing the satellite retrievals with in situ data from field programs and additional PIREPS.

All PIREPS taken within a half hour of 1545 and 2145 UTC over the GOES-12 domain during February 2004 and over the GOES-10 domain from 1 –11 February 2004 were compared with the VISST results. The average cloud properties and icing probabilities were computed for 3 x 3 pixel arrays centered on the position given in each PIREP. The results, based on 4665 matches, are summarized in Table 1 for the cloud properties. Mean cloud *OD*, *LWP*, and thickness all increase with increasing icing intensity and the average cloud temperature is lower for the cases with positive PIREPS icing. The mean effective cloud droplet sizes, however, are not significantly different for icing and no-icing cases. Although the standard deviations are large, especially for LWP, the mean results confirm the LWP basis of the icing probability algorithm. The dependence on *re* appears to be weaker than seen in earlier comparisons, but the temperature dependence seems to be stronger and the cloud thickness means are well separated for icing and no icing cases.

Table 1. Mean VISST cloud properties corresponding to PIREPS icing reports during February 2004.

Icing Intensity	None	Light	Mod/Sev
OD	18.1	34.0	39.1
re (μm)	12.2	11.8	12.4
LWP (gm^{-2})	269	382	460
h (km)	1.41	2.1	2.4
Tc (K)	269	263	263

The PIREPS reported icing in 54.5% of the cases. When the PIREPS reported icing, the satellite algorithm produced 27% icing, 22% indeterminate, and 5.5% no icing relative to the total number of PIREPS. When the PIREPS indicated no icing, the satellite algorithm produced 22.6% no icing, 8.5% indeterminate, and 14.6% positive icing probabilities. Thus, in 5.5% of the cases, the GOES missed the icing (false negatives) while producing 14.6% false positives. Many of the false negatives result from relatively small LWP values and may be affected by the time differences between the satellite image and the PIREP report location. The false positives are the result of using probability estimates and may coincide with some of the aircraft-related factors noted earlier.

Because the indeterminate cases account for 30% of the observations, it is desirable to account for the potential of clouds underneath the ice clouds. The Cloud Icing Potential (CIP) product (Bernstein et al. (2004) already integrates RUC, PIREPS, and ceilometer data to estimate icing probability. Blending the satellite results with the CIP would be an attractive means for taking the indeterminate data into account. For assimilating the products into forecast models, it would be optimal to produce a 3-D dataset by accounting for multilayered clouds. Such an approach would fill out the satellite data in the vertical using multilayered detection methods (e.g., Kawamoto et al., 2002), ceilometer cloud base estimates, and RUC data linked to cloud radar data (Minnis et al., 2004c). This technique for developing a 3-D dataset needs further exploration.

It is critical to properly place the clouds in the right vertical location. For the 855 times when VISST and PIREPS reported icing, the aircraft mean altitude was within the vertical boundaries from VISST in 70% of the cases. The VISST cloud-top height was too high in 26% of the cases and too low 4% of the time.

4. CONCLUDING REMARKS

A preliminary new, physically based method for real-time estimation of the probability of icing conditions has been demonstrated using merged GOES-10 and 12 data over the continental United States and southern Canada. The algorithm produces pixel-level cloud and radiation properties as well as an estimate of icing probability with an associated intensity rating Because icing depends on so many different variables, such as aircraft size or air speed, it is not possible to achieve 100% success with this or any other type of approach. This initial algorithm, however, shows great promise for diagnosing aircraft icing and putting it at the correct altitude within 0.5 km most of the time. Much additional research must be completed before it can serve as a reliable input for the operational CIP. The delineation of the icing layer vertical boundaries will need to be improved using either the RUC or balloon soundings or ceilometer data to adjust the cloud base height, a change that would require adjustment of the cloud-top altitude also.

Only daytime data have been considered so far. While the SIST has demonstrated some skill in discriminating between optically thin and thick clouds at night, the utility of the resulting products for icing classification has not yet been examined. Most of the indeterminate cases were found to be a combination of a high ice clouds over an icing cloud. Better detection of multilayered clouds using multispectral IR data or matched microwave and VIS data over water surfaces (Huang et al., 2004) would help minimize the number of indeterminate cases. Other ways to eliminate the indeterminate cases include using the ceilometer data along with RUC soundings to locate a lower-level cloud deck or, in a more universal approach, using empirical relationships between clouds and the RUC profiles (Yi et al. 2004) to diagnose clouds underneath the satellite-observed cirrus clouds. Similar methods are already being used to develop the current CIP product and could be adapted to work in a conditional probability scenario with the satellite retrievals. False returns caused by thin cirrus clouds over warm, low cloud decks can also be minimized by using the multispectral IR methods to detect thin cirrus clouds. Such techniques typically rely on the 12-μm data, which are currently not available GOES-12. Hopefully, future GOES imagers will return the 13.3-μm channel on GOES-12 to the original 12-μm channel.

The satellite icing algorithms are just one part of a comprehensive aircraft icing program being developed by NASA, NOAA, and the FAA. Ultimately, the results will be combined with PIREPS, model forecasts, and other data within the CIP to provide a near-real time optimized characterization of icing conditions for pilots and flight controllers.

ACKNOWLEDGEMENTS

This research was supported by the NASA Aviation Safety Program through the NASA Advanced Satellite Aviation-weather Products Initiative. Additional support was provided by the Environmental Sciences Division of U.S. Department of Energy Interagency Agreement DE-AI02-97ER62341 through the ARM Program.

REFERENCES

Benjamin, S. G., D. Dévényi, S. S. Weygandt, K. J. Brundage, J. M. Brown, G. A. Grell, D. Kim, B. E. Schwartz, T. G. Smirnova, and T. L. Smith, and G. S. Manikin, 2004: An hourly assimilation-forecast cycle - the RUC. *Mon. Wea. Rev.*, **132**, 495-518.

Bernstein, B.C., F. McDonough, M.K. Politovich and B.G. Brown, 2004: CIP: a physically-based, integrated approach to the diagnosis of in-flight aircraft icing, Part I: Algorithm description. Submitted, *Weather and Forecasting*.

Chakrapani, V., D. R. Doelling, A. D. Rapp, and P. Minnis, 2002: Cloud thickness estimation from GOES-

8 satellite data over the ARM SGP site. *Proc. 12th ARM Science Team Mtg*, April 8-12, St. Petersburg, FL, 14 pp. Available at http://www.arm.gov/docs/documents/technical/conf_0204/chakrapani-v.pdf.

Dong, X., P. Minnis, G. G. Mace, W. L. Smith, Jr., M. Poellot, R. T. Marchand, and A. D. Rapp, 2002: Comparison of stratus cloud properties deduced from surface, GOES, and aircraft data during the March 2000 ARM Cloud IOP. *J. Atmos. Sci.*, **59**, 3256-3284.

Huang, J., P. Minnis, B. Lin, Y. Yi, M. M. Khaiyer, R. F. Arduini, and G. G. Mace, 2004: Advanced retrievals of multilayered cloud properties using multi-sensor and multi-spectral measurements. Accepted, *J. Geophys. Res.*, 10.1029/2004JD005101.

Kawamoto, K., P. Minnis, W. L. Smith, Jr., and A. D. Rapp, 2002: Detecting multilayer clouds using satellite solar and IR channels. *Proc. 11th AMS Conf. Cloud Physics.*, Ogden, UT, June 3-7, CD-ROM, JP1.18.

Min, Q, P. Minnis, and M. M. Khaiyer, 2004: Comparison of cirrus optical depths from GOES-8 and surface measurements. *J. Geophys. Res.*, **109**, D15, D15207 10.1029/2003JD004390.

Minnis, P., D. P. Garber, D. F. Young, R. F. Arduini, and Y. Takano, 1998: Parameterization of reflectance and effective emittance for satellite remote sensing of cloud properties. *J. Atmos. Sci.*, **55**, 3313-3339.

Minnis, P., et al., 1995: Cloud Optical Property Retrieval (Subsystem 4.3). "Clouds and the Earth's Radiant Energy System (CERES) Algorithm Theoretical Basis Document, Volume III: Cloud Analyses and Radiance Inversions (Subsystem 4)", *NASA RP 1376 Vol. 3*, pp. 135-176.

Minnis, P., L. Nguyen, D. R. Doelling, D. F. Young, W. F. Miller, and D. P. Kratz, 2002: Rapid calibration of operational and research meteorological satellite imagers, Part I: Evaluation of research satellite visible channels as references. *J. Atmos. Oceanic Technol.*, **19**, 1233-1249.

Minnis, P., et al., 2001: A near-real time method for deriving cloud and radiation properties from satellites for weather and climate studies. *Proc. AMS 11th Conf. Satellite Meteorology and Oceanography*, Madison, WI, Oct. 15-18, 477-480.

Minnis, P., W. L. Smith, Jr., L. Nguyen, M. M. Khaiyer, D. A. Spangenberg, P. W. Heck, R. Palikonda, B. C. Bernstein, and F. McDonough, 2004b: A real-time satellite-based icing detection system. *Proc. 14th Intl. Conf. Clouds and Precipitation*, Bologna, Italy, 18-23 July.

Minnis, P., Y. Yi, J. Huang, and J. K. Ayers, 2004: Relationships between meteorological conditions and cloud properties determined from ARM data. Submitted *J. Geophys. Res.*

Minnis, P., D. F. Young, S. Sun-Mack, Q. Z. Trepte, R. R. Brown, S. Gibson, and P. Heck, 2004a: Diurnal, seasonal, and interannual variations of cloud properties derived for CERES from imager data. *Proc. 13th AMS Conf. Satellite Oceanogr. and Meteorol.*, Norfolk, VA, Sept. 20-24, CD-ROM, P6.10.

Smith, W. L., Jr., P. Minnis, B. C. Bernstein, A. D. Rapp, and P. W. Heck, 2002: Supercooled liquid water cloud properties derived from GOES: Comparisons with in situ aircraft measurements. *10tth AMS Conf. Aviation, Range, and Aerospace Meteorol.*, Portland, OR, May 13-16, 89-92.

Smith, W. L., Jr., P. Minnis, B. C. Bernstein, F. McDonough, and M. M. Khaiyer, 2003: Comparison of supercooled liquid water cloud properties derived from satellite and aircraft measurements. *Proc. FAA In-Flight Icing/De-icing International Conference*, Chicago, IL, June 16-20, CD_ROM, 2003-01-2156.

Smith, W. L., Jr., P. Minnis, and D. F. Young, An icing product derived from operational satellite data. *Proc. AMS 9th Conf. Aviation, Range, and Aerospace Meteorol.*, Orlando, FL, 11-15 Sept., 256-259, 2000.

Yi, Y., P. Minnis, J. Huang, and J. K. Ayers, 2004: Cloud detection using measured and modeled statge parameters. *Proc. 13th AMS Conf. Satellite Oceanogr. and Meteorol.*, Norfolk, VA, Sept. 20-24, CD-ROM, P6.11.

Young, D. F., P. Minnis, D. Baumgardner, and H. Gerber, 1998: Comparison of in situ and satellite-derived cloud properties during SUCCESS. *Geophys. Res. Lett.*, **25**, 1125-1128.